BMC Plant Biology

RESEARCH

Open Access

Identification of key modules and genes in response to high-temperature stress in *Platostoma palustre* based on WGCNA

Xiufang Li[1,2†], Wei Fan[1†], Changqian Quan[1], Meihua Xu[1] and Danfeng Tang[1,3*]

Abstract

Platostoma palustre (Blume) A. J. Paton is one of the important medicinal and edible plants in China, and it is widely cultivated in tropical and subtropical regions of southern China. In these areas, high-temperature stress (HTS) is often one of the unfavorable environmental factors affecting the growth and yield of *P. palustre*. Nevertheless, the molecular mechanism underlying the response of *P. palustre* to HTS remains unclear. In this study, we used two varieties of *P. palustre*, LSL and MDG, as experimental materials to identify key genes involved in the response of *P. palustre* to HTS by employing transcriptome sequencing technology, thereby revealing the molecular mechanism underlying its adaptation to HTS. The results showed that HTS significantly influenced the plant height, above-ground fresh weight, root fresh weight, root growth, chlorophyll a, chlorophyll b, chlorophyll a + b, and carotenoid content of *P. palustre* plants. MDG exhibited stronger high-temperature tolerance compared to LSL. Under HTS, 8352 DEGs were up-regulated and 9201 DEGs were down-regulated in HT_LSL_vs_CK_LSL, while 5433 DEGs were up-regulated and 6325 DEGs were down-regulated in HT_MDG_vs_CK_MDG, suggesting a significant difference in gene expression levels between LSL and MDG under HTS. KEGG enrichment analysis showed the pathways possibly involved in HTS responses in *P. palustre*, such as plant hormone signal transduction, brassinosteroid biosynthesis, phenylpropanoid biosynthesis, pentose and glucuronate interconversions, diterpenoid biosynthesis, flavonoid biosynthesis, etc. Further weighted gene co-expression network analysis (WGCNA) identified 14 modules and 61 hub genes closely related to the response to HTS in *P. palustre*. The hub genes included peroxidase 51-like (*TRINITY_DN34017_c0_g1*), UDP-glucuronate 4-epimerase 1-like (GAE1, *TRINITY_DN815_c0_g3*), NAC domain-containing protein 1 (NAC, *TRINITY_DN328_c0_g1*), UGT73A13 (*TRINITY_DN8437_c0_g2*), universal stress protein 7 (USP7, *TRINITY_DN6361_c0_g2*), malonyl-coenzyme: anthocyanin 5-O-glucoside-6‴-O-malonyltransferase-like (5MaT1, *TRINITY_DN3589_c0_g1*), ent-kaurene synthase 5 (KSL5, *TRINITY_DN5126_c0_g1*), ABC transporter (*TRINITY_DN39495_c0_g1*, *TRINITY_DN10383_c0_g1*), etc. This study investigated the molecular mechanism of heat tolerance in *P. palustre* at the gene expression level, providing a scientific basis for heat-tolerant breeding of *P. palustre*.

Keywords *Platostoma palustre* (Blume) A. J. Paton, High-temperature stress, Physiological and biochemical indicators, Transcriptome, WGCNA

†Xiufang Li and Wei Fan contributed equally to this work.

*Correspondence:
Danfeng Tang
tdfmanuscript@163.com
[1]Guangxi Key Laboratory of Medicinal Resources Protection and Genetic Improvement/Guangxi Engineering Research Center of TCM Resource Intelligent Creation, National Center for TCM Inheritance and Innovation, Guangxi Botanical Garden of Medicinal Plants, Nanning 530023, China
[2]College of Pharmacy, Guangxi Medical University, Nanning 530200, China
[3]National Engineering Research Center for Southwest Endangered Medicinal Materials Resources Development, Guangxi Botanical Garden of Medicinal Plants, Nanning 530023, China

Introduction

Platostoma palustre (Blume) A. J. Paton, also known as "Liangfencao" or "Xiancao" in Chinese, belongs to the Platostoma genus within the Lamiaceae family [1, 2]. According to the Flora of China (http://www.iplant.cn/info/Platostoma%20palustre), it is distributed in regions such as Taiwan, Zhejiang, Jiangxi, Guangdong, and western Guangxi in China [3]. *P. palustre* is an important plant resource for both medicinal and edible use, possessing functions of clearing summer heat, cooling the blood, and detoxifying [4, 5]. It can be used to make unique summer delicacies such as jelly, herbal tea, cola, and other botanical beverages, as well as various health foods [6, 7]. *P. palustre* contains multiple active ingredients, including polysaccharides, triterpenes, flavonoids, phenols, and other compounds, which exhibit various biological activities such as antioxidant, hypotensive, hypolipidemic, and antibacterial effects [8]. Therefore, as a plant resource with both medicinal and edible values, *P. palustre* has seen its deep-processed products (particularly herbal tea) gain significant market popularity, and it has consequently become a research focus [9, 10].

As global climate anomalies intensify, the frequency and number of extreme weather events such as high temperatures, droughts, and floods have gradually increased, posing increasingly severe threats to agricultural production. Currently, high temperatures and droughts are recognized as the two major abiotic stress factors, leading to crop yield reductions and even total crop failures [11, 12]. High-temperature stress (HTS) is a common abiotic stress encountered during plant growth and development, which disrupts plant metabolism by degrading proteins, thereby causing growth and development retardation [13]. HTS can cause necrosis and chlorophyll loss on the edges and tips of plant leaves, premature senescence and abscission of leaves, flowers, and fruits, inhibition of root and bud growth, and so on [14]. Plants exhibit different sensitivities to HTS at different phenological stages, and there are also differences among different species and different genotypes within the same species.

P. palustre prefers shady and moist environments and is relatively intolerant of prolonged droughts. It grows well within a temperature range of 15–35 °C [15]. If the temperature exceeds 20 °C, the growth rate is extremely fast. Conversely, if the temperature is below 20 °C, the growth rate significantly slows down; below 10 °C, growth basically ceases; and around 0 °C, the stems and leaves wilt, but the roots remain viable in the soil. Therefore, ensuring adequate rainfall and moderate temperature and humid conditions is very beneficial for the growth of *P. palustre* [16]. At present, the main cultivation areas of *P. palustre* are mostly in southern China and Southeast Asian countries. These regions experience high temperatures during summer, and plants are highly susceptible to heat stress during cultivation, which can lead to decreased disease resistance, slowed growth, and even reduced yields or crop failures. Therefore, screening for heat-tolerant varieties of *P. palustre* is one of the important research directions, and studying the mechanism of heat tolerance in *P. palustre* becomes particularly crucial.

Currently, there have been no reports on the molecular mechanism of how *P. palustre* responds to high-temperature stress. Therefore, this study used two varieties of *P. palustre* (LSL and MDG, originating from Guangxi and Guangdong respectively, exhibit differential stress resistance based on preliminary observations) as experimental materials. Through high-temperature stress experiments and employing transcriptome sequencing technology, we analyzed the changes in gene expression under high-temperature stress in *P. palustre*. This study aims to investigate the molecular mechanism of heat tolerance in *P. palustre* at the transcriptional level, providing a scientific basis for heat-tolerant breeding of *P. palustre*.

Results

HTS affected the growth of *P. palustre* plants

High-temperature stress significantly influenced the plant height, above-ground fresh weight, and root fresh weight of *P. palustre* plants (Figs. 1 and 2). Compared to the control (a diurnal temperature of 28 °C/26°C), LSL exhibited reductions of 20.68% in plant height, 52.66% in above-ground fresh weight, and 44.68% in root fresh weight under high-temperature stress conditions (a diurnal temperature of 38 °C/32°C). Similarly, MDG showed decreases of 20.90% in plant height, 26.71% in above-ground fresh weight, and 41.66% in root fresh weight under high-temperature stress. Additionally, high-temperature stress also affected the root growth of *P. palustre* plants (Fig. 3). LSL demonstrated significant reductions in root length, root surface area, and average root diameter, with decreases of 19.55%, 24.27%, and 15.17%, respectively compared to the control. In contrast, only the average root diameter of MDG was significantly decreased by 10.67% compared to the control.

HTS affected the photosynthetic pigment content of *P. palustre*

High-temperature stress had no significant effect on the chlorophyll a (Chla), chlorophyll b (Chlb), chlorophyll a + b (Chla + b), and carotenoid (Car) content of MDG compared to the control group. However, high-temperature stress had a significant impact on the chlorophyll a, chlorophyll a + b, and carotenoid content of LSL, with reductions of 35.02%, 31.71%, and 33.26%, respectively, compared to the control (Fig. 4).

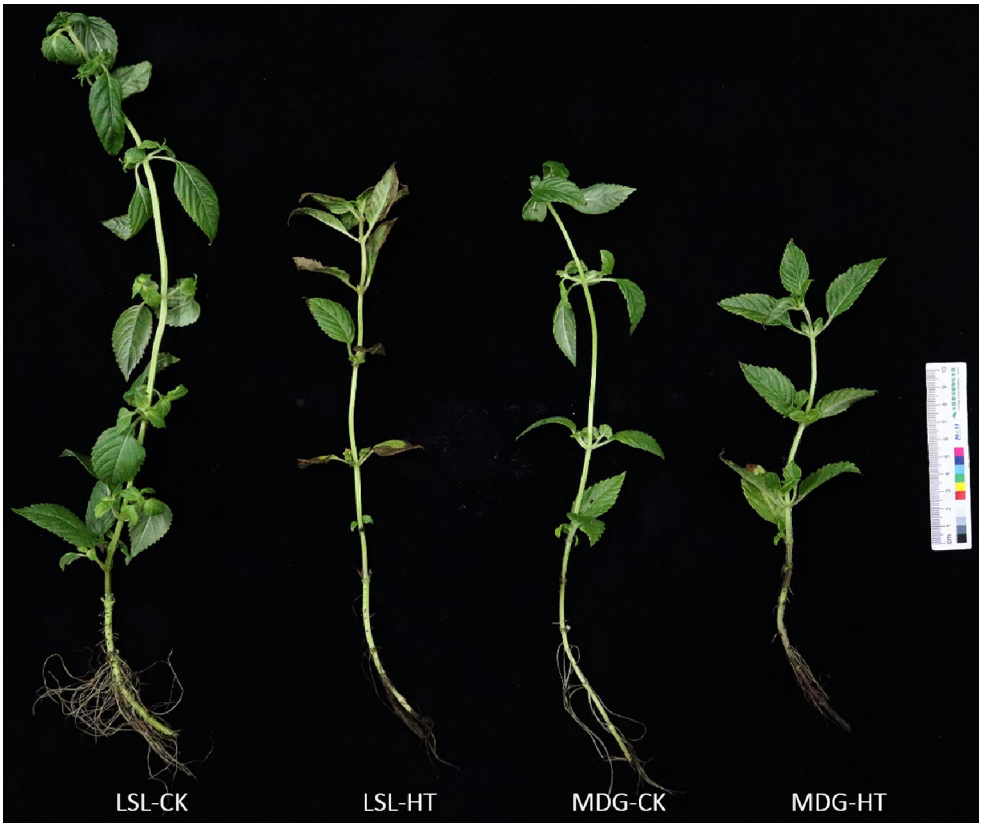

Fig. 1 Comparison of the morphology of *P. palustre* plants under high temperature and control conditions

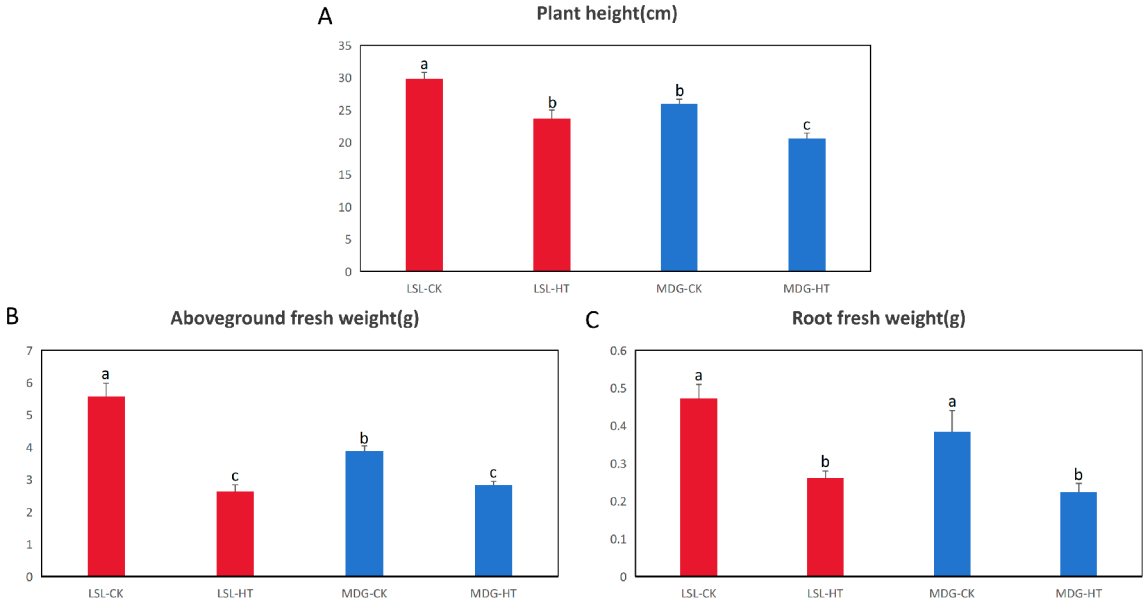

Fig. 2 High-temperature stress affected the growth of *P. paluste* plants. (**A**) Plant height. (**B**) Aboveground fresh weight. (**C**) Root fresh weight

Quality assessment and functional annotation of RNA-seq data

In this study, we performed transcriptome sequencing on 12 samples across four treatments (HT_LSL, HT_MDG, CK_LSL, and CK_MDG), with three replicates per treatment. The results indicated that a total of 89.41 Gb of clean data was obtained, with each sample generating over 6.7 Gb of clean data. The Q20 base percentage exceeded 98.02%, the Q30 base percentage exceeded

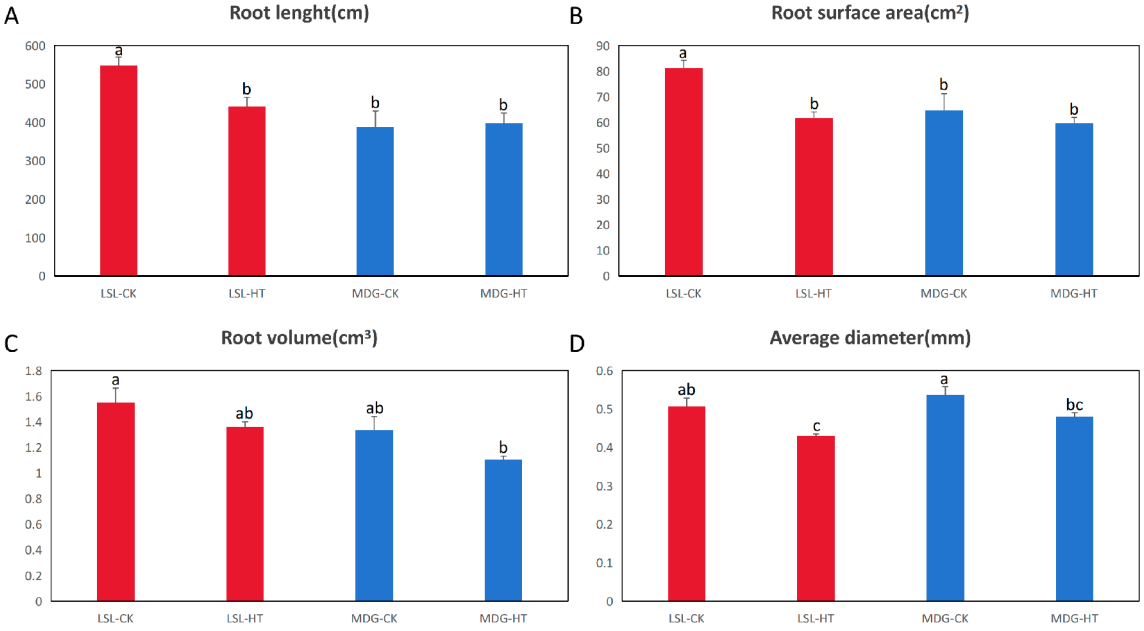

Fig. 3 High-temperature stress affected the root system of *P. palustre* plants. (**A**) Root length. (**B**) Root surface area. (**C**) Root volume. (**D**) Average diameter

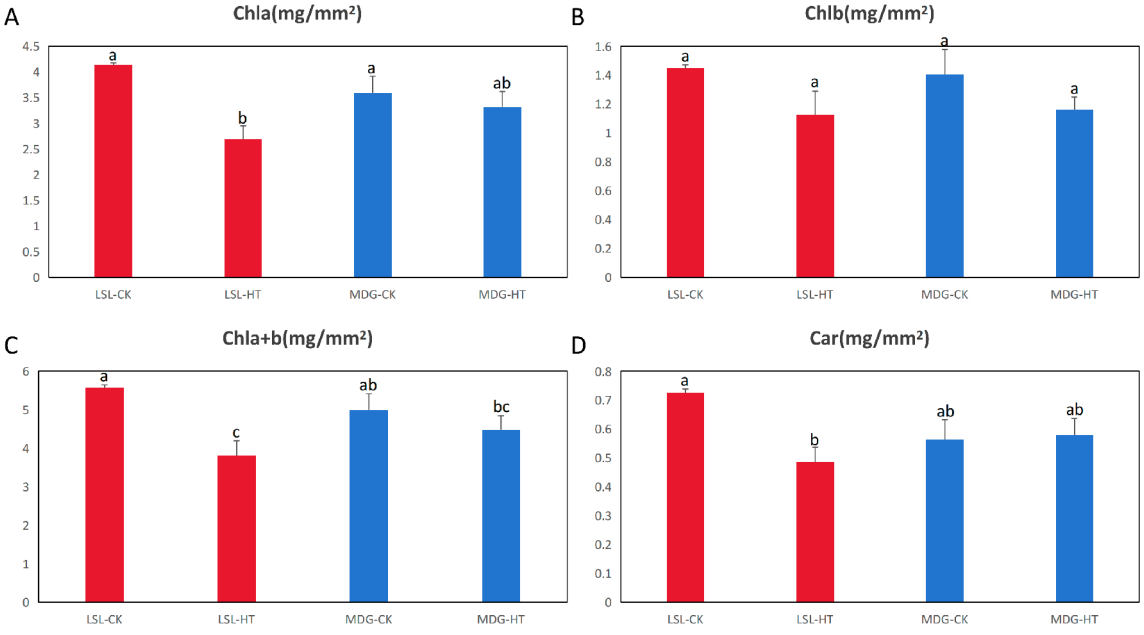

Fig. 4 High-temperature stress affected the photosynthetic pigment content of *P. palustre*. (**A**) Chla. (**B**) Chlb. (**C**) Chla + b. (**D**) Car

94.17%, and the GC content ranged from 45.05 to 45.77% (Table 1).

This study obtained 94,903 unigenes and 172,374 transcripts. The average length of unigenes was 939.68 bp, with an N50 length of 1516 bp. Similarly, the average length of transcripts was 1134.54 bp, with an N50 length of 1779 bp (Table S1). The analysis of transcript length distribution revealed that the majority of unigenes (42,207, 44%) had sequence lengths ranging from 200 to 500 bp (Figure S1). The clean reads from each sample were aligned to the Trinity-assembled reference sequences to obtain mapping results, with mapping ratios ranging from 74.59 to 77.79% (Table S2). The unigenes and transcripts obtained from transcriptome assembly were compared with six major databases (NR, Swiss-Prot, Pfam, EggNOG, GO, and KEGG) to comprehensively annotate their functional information. The annotation status of each database was statistically analyzed (Figure S2, S3).

Table 1 Transcriptome sequencing data statistics and quality evaluation

Sample	Raw reads	Raw bases(bp)	Clean reads	Clean bases(bp)	Error rate(%)	Q20(%)	Q30(%)	GC content(%)
CK_LSL_1	53127040	8022183040	52192382	7846710475	0.025	98.03	94.22	45.77
CK_LSL_2	45914340	6933065340	45142288	6789302949	0.0248	98.07	94.33	45.65
CK_LSL_3	52690258	7956228958	51852480	7801007078	0.0248	98.1	94.39	45.63
HT_LSL_1	53868648	8134165848	53010556	7969254079	0.0247	98.13	94.48	45.06
HT_LSL_2	45280536	6837360936	44554544	6701259823	0.0248	98.08	94.34	45.09
HT_LSL_3	49538616	7480331016	48754284	7331285861	0.025	98.02	94.17	45.05
CK_MDG_1	51348086	7753560986	50458650	7591236006	0.0246	98.16	94.59	45.42
CK_MDG_2	53873356	8134876756	52973294	7948908820	0.0248	98.09	94.4	45.4
CK_MDG_3	52555178	7935831878	51794384	7791935001	0.0246	98.16	94.55	45.36
HT_MDG_1	46740388	7057798588	46076440	6933464217	0.0246	98.17	94.54	45.41
HT_MDG_2	51379712	7758336512	50689504	7627018197	0.0245	98.19	94.64	45.43
HT_MDG_3	47704238	7203339938	46981074	7074095848	0.0249	98.04	94.24	45.44

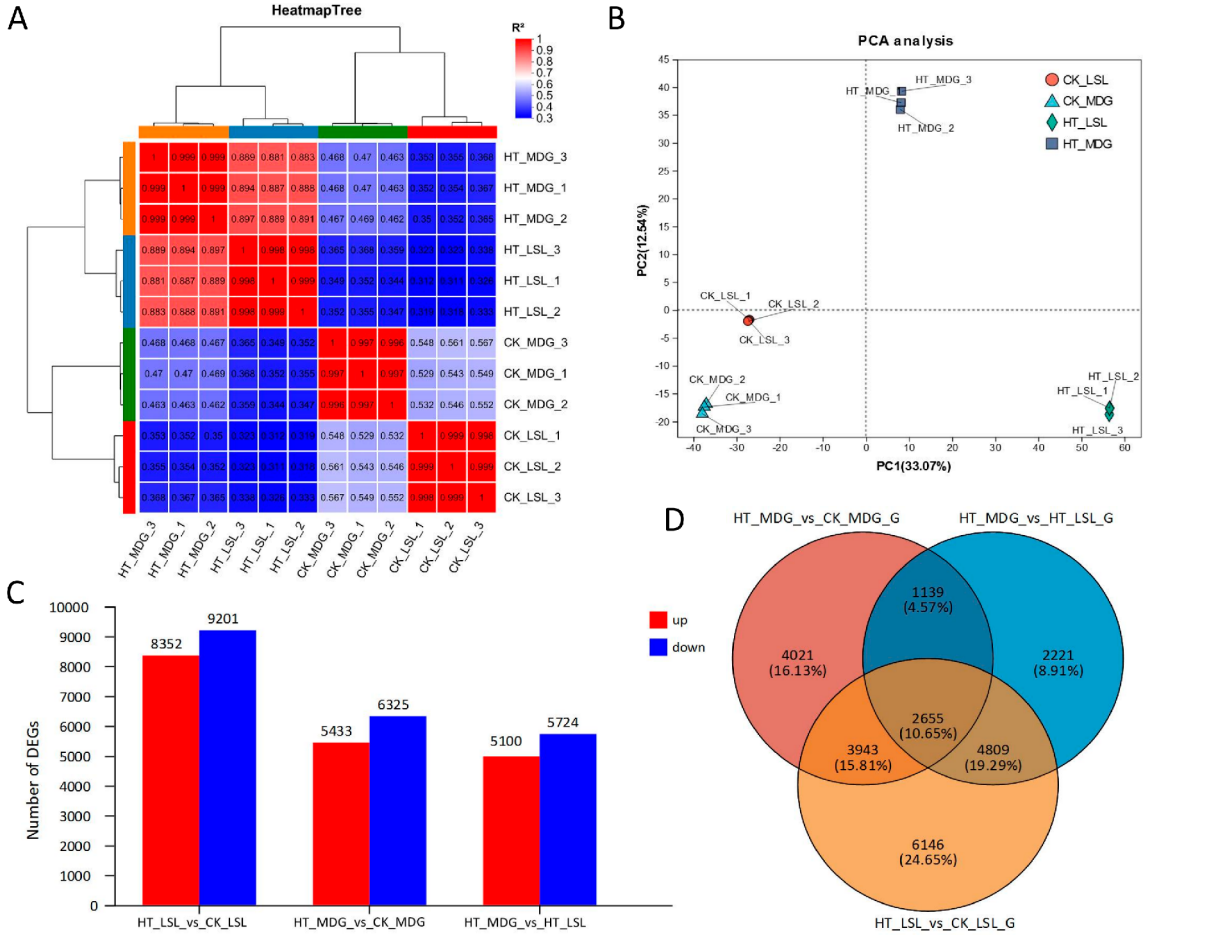

Fig. 5 Statistical analysis of RNA sequencing data. (**A**) Correlation analysis of samples. (**B**) PCA analysis. (**C**) DEG statistical analysis. (**D**) Venn analysis of different comparison groups

Analysis of DEGs

The RSEM software package was utilized for quantitative analysis of unigene/transcript expression levels, yielding TPM (Transcripts Per Million) values and read counts. The statistical analysis revealed that the Pearson correlation coefficient confirmed biological consistency (Fig. 5A). Furthermore, PCA analysis demonstrated significant differences in gene cluster expression between the control group (CK_LSL, CK_MDG) and the high-temperature treatment group (HT_LSL, HT_MDG) (Fig. 5B). Under high-temperature stress, 8352 DEGs were up-regulated and 9201 DEGs were down-regulated in HT_LSL_vs_CK_LSL, while 5433 DEGs were up-regulated and 6325 DEGs were down-regulated in

HT_MDG_vs_CK_MDG (Fig. 5C). There were 5100 up-regulated and 5724 down-regulated DEGs in HT_LSL_vs_HT_MDG (Fig. 5C). Notably, after high-temperature stress, the number of up-regulated and down-regulated DEGs in LSL was significantly higher than that in MDG, suggesting a significant difference in gene expression levels between the two varieties under high-temperature stress. Additionally, a total of 2655 DEGs were identified across three comparison groups, HT_LSL_vs_CK_LSL, HT_MDG_vs_CK_MDG, and HT_MDG_vs_HT_LSL. These findings indicated that the expression of these genes may be induced in response to high-temperature stress irrespective of the genotype (Fig. 5D).

Transcription factor (TF) analysis

In this study, we identified a total of 1,352 TFs in both LSL and MDG. The *MYB_superfamily* accounted for the highest percentage (202 TFs), followed by *AP2/ERF* (157 TFs) and *C2C2* (118 TFs) (Figure S4). In the HT_LSL_vs_CK_LSL comparison group (Fig. 6A), the *MYB_superfamily* had the highest percentage of differentially expressed TFs (15.78%), followed by *AP2/ERF* (13.48%), *bHLH family* (9.57%), HSF family (1.95%), etc. In the HT_MDG_vs_CK_MDG comparison group (Fig. 6B), the *MYB_superfamily* also had the highest percentage of differentially expressed TFs (15.51%), followed by *AP2/ERF* (14.68%), *bHLH* (10.48%), HSF family (2.94%), etc. In the HT_MDG_vs_HT_LSL comparison group (Fig. 6C), the *MYB_superfamily* still had the highest percentage of differentially expressed TFs (14.07%), followed by *AP2/ERF* (12.31%), *NAC* (9.80%), HSF family (1.76%), etc. Generally, under high-temperature stress conditions, the types and numbers of differentially expressed TFs varied minimally among the different comparison groups.

GO enrichment analysis of DEGs

We performed GO enrichment analysis of DEGs in different comparison groups (Fig. 7). In the HT_LSL_vs_CK_LSL comparison group, the DEGs were primarily enriched in the GO terms such as plasma membrane, extracellular region, monooxygenase activity, phenylpropanoid metabolic process, secondary metabolic process, cell wall organization or biogenesis, etc. (Fig. 7A). In the HT_MDG_vs_CK_MDG comparison group, the DEGs were mainly enriched in the GO terms like plasma membrane, extracellular region, monooxygenase activity, phenylpropanoid metabolic process, secondary metabolic process, cell wall organization or biogenesis, etc. (Fig. 7B). In the HT_MDG_vs_HT_LSL comparison group, the DEGs were predominantly enriched in the GO terms, for example, plasma membrane, extracellular region, monooxygenase activity, response to biotic stimulus, response to stimulus, response to external stimulus, etc. (Fig. 7C).

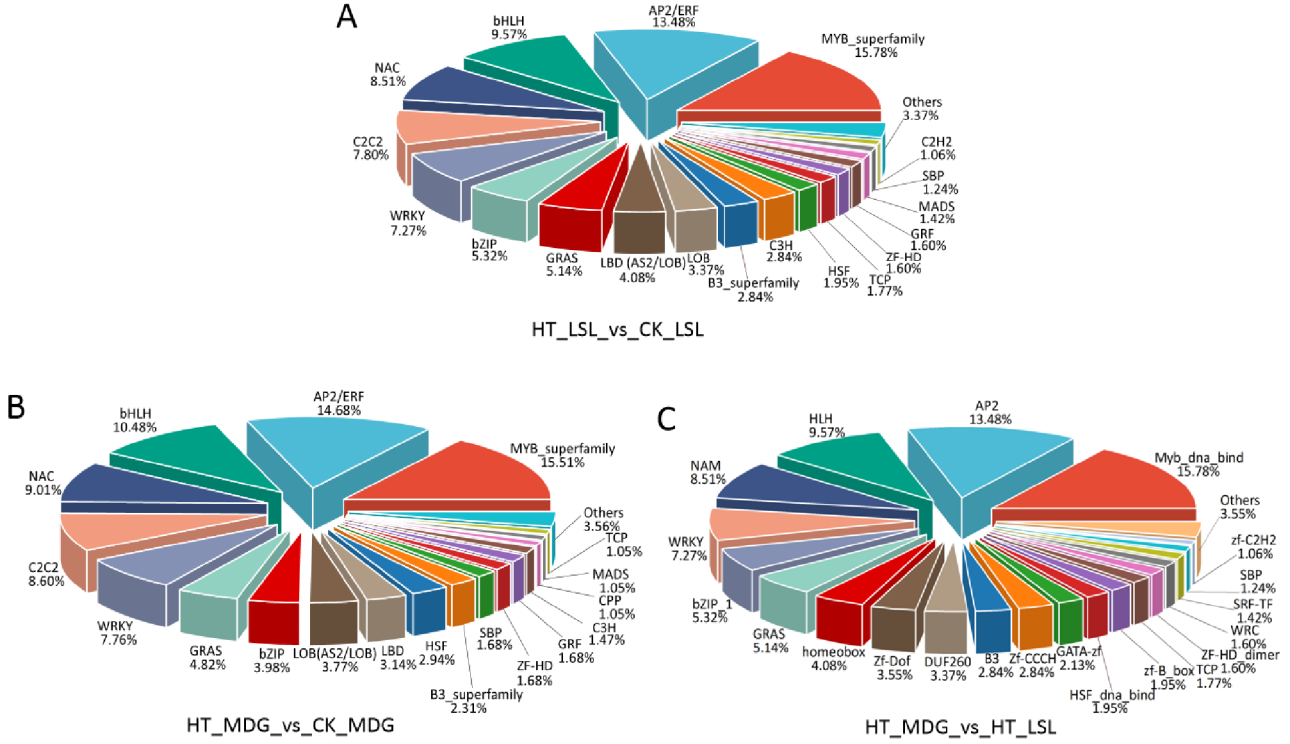

Fig. 6 TF analysis. (**A**) TF analysis in HT_LSL_vs_CK_LSL comparison group. (**B**) TF analysis in HT_MDG_vs_CK_MDG comparison group. (**C**) TF analysis in HT_MDG_vs_HT_LSL comparison group

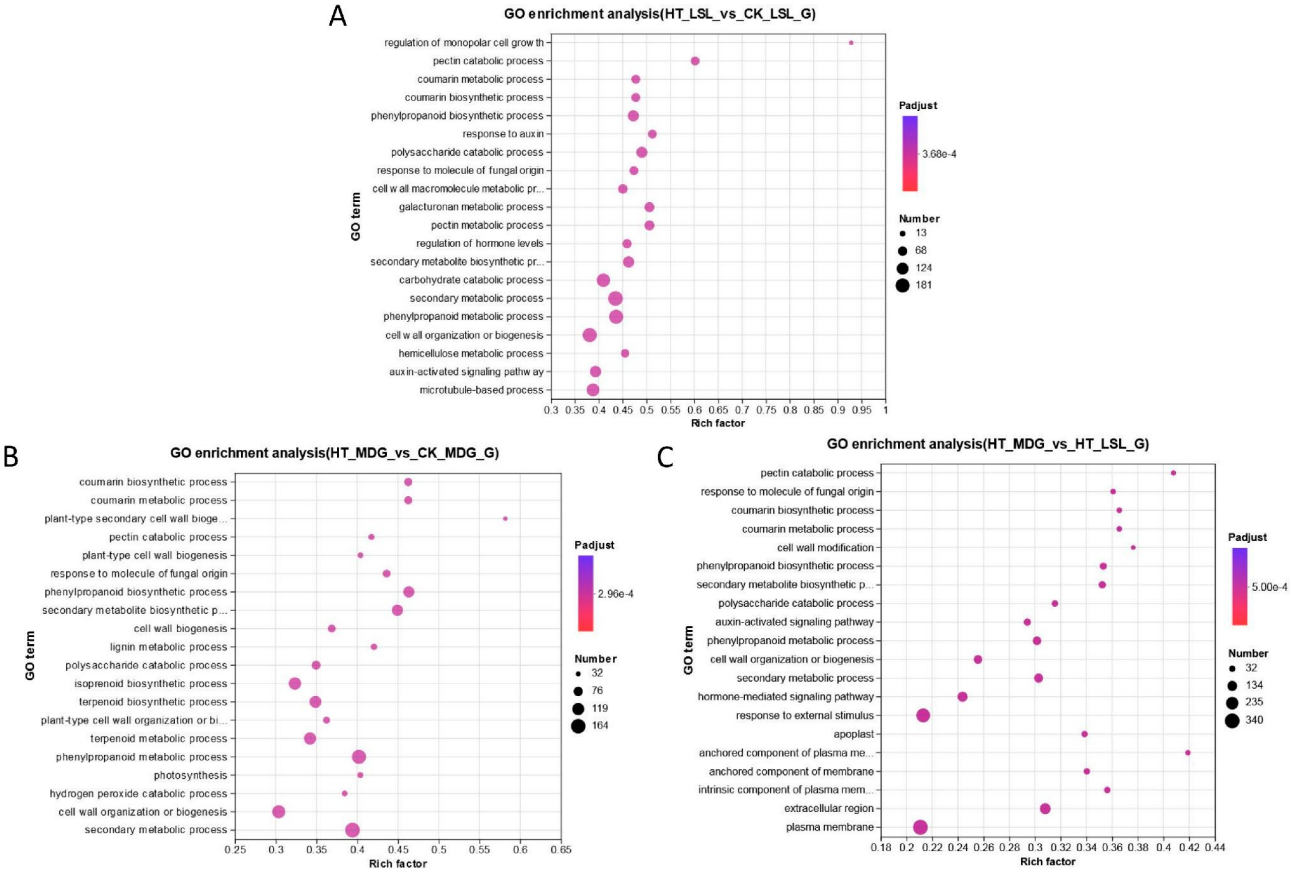

Fig. 7 GO enrichment analysis. (**A**) GO enrichment analysis in HT_LSL_vs_CK_LSL comparison group. (**B**) GO enrichment analysis in HT_MDG_vs_CK_MDG comparison group. (**C**) GO enrichment analysis in HT_MDG_vs_HT_LSL comparison group

KEGG enrichment analysis of DEGs

We further performed KEGG enrichment analysis of DEGs in different comparison groups (Fig. 8). In the HT_LSL_vs_CK_LSL comparison group (Fig. 8A), DEGs were significantly enriched in pathways such as phenylpropanoid biosynthesis, diterpenoid biosynthesis, pentose and glucuronate interconversions, plant hormone signal transduction, galactose metabolism, and so on. In the HT_MDG_vs_CK_MDG comparison group (Fig. 8B), DEGs were significantly enriched in pathways such as phenylpropanoid biosynthesis, plant hormone signal transduction, flavonoid biosynthesis, carbon fixation in photosynthetic organisms, diterpenoid biosynthesis, etc. In the HT_MDG_vs_HT_LSL comparison group (Fig. 8C), DEGs were significantly enriched in pathways such as phenylpropanoid biosynthesis, pentose and glucuronate interconversions, plant hormone signal transduction, alpha-Linolenic acid metabolism, valine, leucine and isoleucine degradation, brassinosteroid biosynthesis, etc. Among the three comparison groups, a total of 12 significantly enriched pathways were found, including plant hormone signal transduction, brassinosteroid biosynthesis, phenylpropanoid biosynthesis, pentose and glucuronate interconversions, diterpenoid biosynthesis, flavonoid biosynthesis, etc. (Fig. 8D, Table S3). It was inferred that these pathways might be involved in heat temperature stress responses in *P. palustre*.

Weighted gene co-expression network analysis

Using WGCNA, various physiological and biochemical indicators were analyzed, and a total of 14 modules were identified. Among them, the turquoise module contained the largest number of genes (Fig. 9A-C). Additionally, the correlation between each module and each indicator was analyzed (Fig. 9D). The module analysis results showed that plant height, aboveground fresh weight, root fresh weight, and chlorophyll b were most closely related to the brown module, with correlation coefficients of -0.93 ($P = 0.00001$), -0.881 ($P = 0.00015$), -0.699 ($P = 0.0114$), and -0.762 ($P = 0.00397$), respectively. By setting MM > 0.8 and|GS|>0.8, module genes closely related to plant height, aboveground fresh weight, and chlorophyll b were screened, with 621, 802, and 320 related genes identified, respectively. For root fresh weight, the parameters were set as MM > 0.8 and|GS|>0.7, resulting in the screening of 357 genes. Further screening for the top 30 genes in terms of connectivity within the co-expression network was conducted to identify hub genes. The results showed

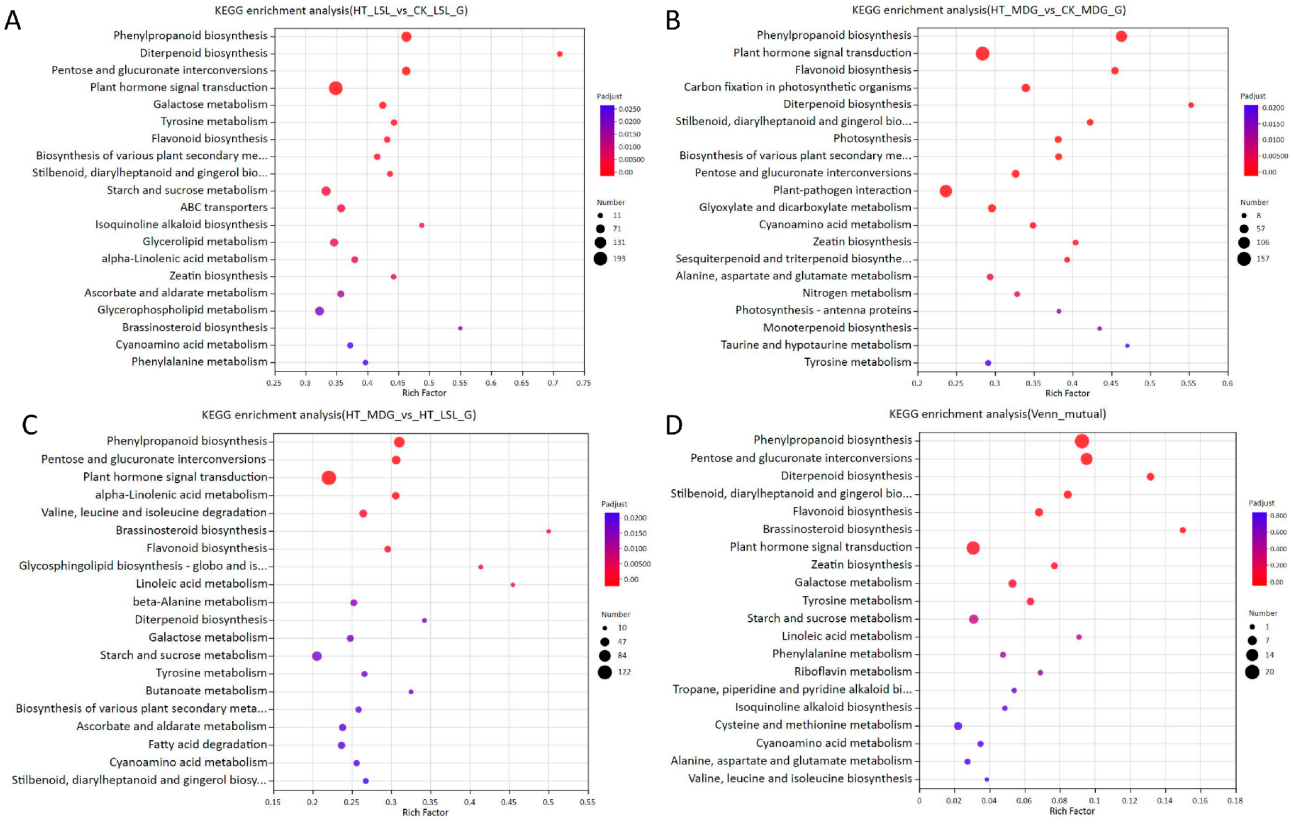

Fig. 8 KEGG enrichment analysis. (**A**) KEGG enrichment analysis in HT_LSL_vs_CK_LSL comparison group. (**B**) KEGG enrichment analysis in HT_MDG_vs_CK_MDG comparison group. (**C**) KEGG enrichment analysis in HT_MDG_vs_HT_LSL comparison group. (**D**) KEGG enrichment analysis in the three comparison groups

that there were 19, 10, 5, and 4 hub genes related to plant height, aboveground fresh weight, root fresh weight, and chlorophyll b, respectively (Fig. 10A-D). Chlorophyll a, total chlorophyll, and carotenoids were most closely related to the greenyellow module, with correlation coefficients of 0.818 ($P = 0.00115$), 0.734 ($P = 0.00657$), and 0.79 ($P = 0.00223$), respectively. By setting MM > 0.8 and|GS|>0.7, the number of related genes for chlorophyll a, total chlorophyll, and carotenoids were screened to be 78, 36, and 48, respectively. Further screening for hub genes under the same conditions yielded 13, 6, and 7 hub genes, respectively (Fig. 10E-G). Root volume, average root diameter, and root length were most closely related to the red, turquoise, and magenta modules, with correlation coefficients of -0.65 ($P = 0.0221$), 0.846 ($P = 0.0005$), and 0.699 ($P = 0.0114$), respectively. Further screening for module genes was conducted, with parameters set as MM > 0.8 and|GS|>0.7 for root volume and root length, and MM > 0.8 and|GS|>0.8 for average root diameter. The final number of genes related to root volume, average root diameter, and root length was 65, 700, and 75, respectively. Similarly, the top 30 genes in terms of connectivity within the co-expression network were screened as hub genes, resulting in 8, 5, and 14 hub genes related to root volume, average root diameter, and root length, respectively (Fig. 10H-J).

Overall, WGCNA identified 61 hub genes closely related to different traits, which may be involved in the response to high-temperature stress in *P. palustre*, including peroxidase 51-like (*TRINITY_DN34017_c0_g1*), UDP-glucuronate 4-epimerase 1-like (GAE1, *TRINITY_DN815_c0_g3*), NAC domain-containing protein 1 (NAC, *TRINITY_DN328_c0_g1*), UGT73A13 (*TRINITY_DN8437_c0_g2*), universal stress protein 7 (USP7, *TRINITY_DN6361_c0_g2*), malonyl-coenzyme: anthocyanin 5-O-glucoside-6‴-O-malonyltransferase-like (5MaT1, *TRINITY_DN3589_c0_g1*), ent-kaurene synthase 5 (KSL5, *TRINITY_DN5126_c0_g1*), ABC transporter (*TRINITY_DN39495_c0_g1*, *TRINITY_DN10383_c0_g1*), etc. (Fig. 11, Table S4).

qPCR validation

In this study, based on the result of WGCNA, we selected seven unigenes (*TRINITY_DN34017_c0_g1*, *TRINITY_DN815_c0_g3*, *TRINITY_DN328_c0_g1*, *TRINITY_DN8437_c0_g2*, *TRINITY_DN6361_c0_g2*, *TRINITY_DN3589_c0_g1*, and *TRINITY_DN5126_c0_g1*) for qPCR validation. The results showed that the

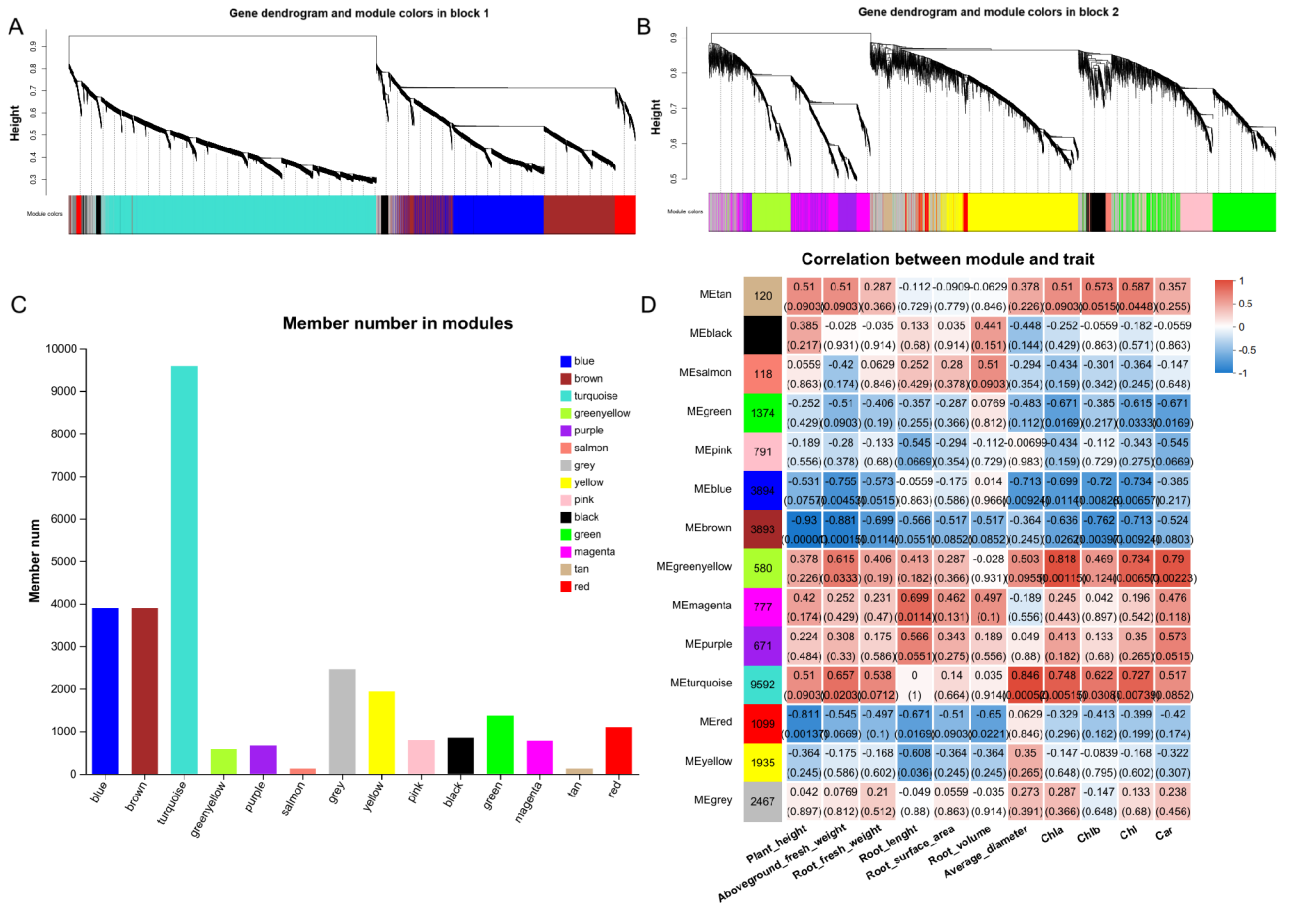

Fig. 9 WGCNA. (**A**) Gene dendrogram and module colors in block (1) (**B**) Gene dendrogram and module colors in block (2) (**C**) Gene member number in modules. (**D**) Correlation between trait and module

expression changes of seven unigenes were in line with those of the transcriptome data (Table S5).

Discussion

High-temperature stress affected the growth and development of *P. palustre* plants

Heat stress refers to temperatures that have a thermal injury effect on plants [17]. Temperatures are considered high when the daily maximum temperature exceeds 35 °C [18]. Continuous high temperatures, defined as daily maximum temperatures of ≥ 35 °C lasting for three or more consecutive days during the growth period, can cause irreversible damage to plant growth and development [19]. Short-term exposure to high-temperature stress can cause plant leaves to lose their chlorophyll and turn yellow, undergo dehydration and wilting, and develop spots on the leaf surface. Prolonged high-temperature stress can lead to the leaves drying up and falling off, stems losing water and shrinking, root rot, and even the entire plant drying up and dying [20, 21]. The configuration and vitality of the root system directly affect the growth and development of the aboveground parts as well as yield formation [22]. Under high-temperature stress, roots become shorter and thinner, with a significant reduction in biomass [23]. In this study, high-temperature stress significantly influenced the plant height, above-ground fresh weight, root fresh weight, and root growth of *P. palustre* plants (Figs. 2, 3 and 4). These findings were generally consistent with the results mentioned earlier. However, under high-temperature stress, the decrease in growth indices and photosynthetic pigment content of MDG plants was significantly lower than that of LSL, especially as high temperature had no significant effect on the photosynthetic pigment content of MDG. This suggested that MDG may have better heat tolerance than LSL.

Transcriptional expression response of *P. palustre* to high-temperature stress

High temperatures in summer are a major constraint affecting the vegetative growth of *P. palustre*, but there have been no reports on how it responds to high-temperature stress at the transcriptional level. Using transcriptome sequencing technology can enable the exploration

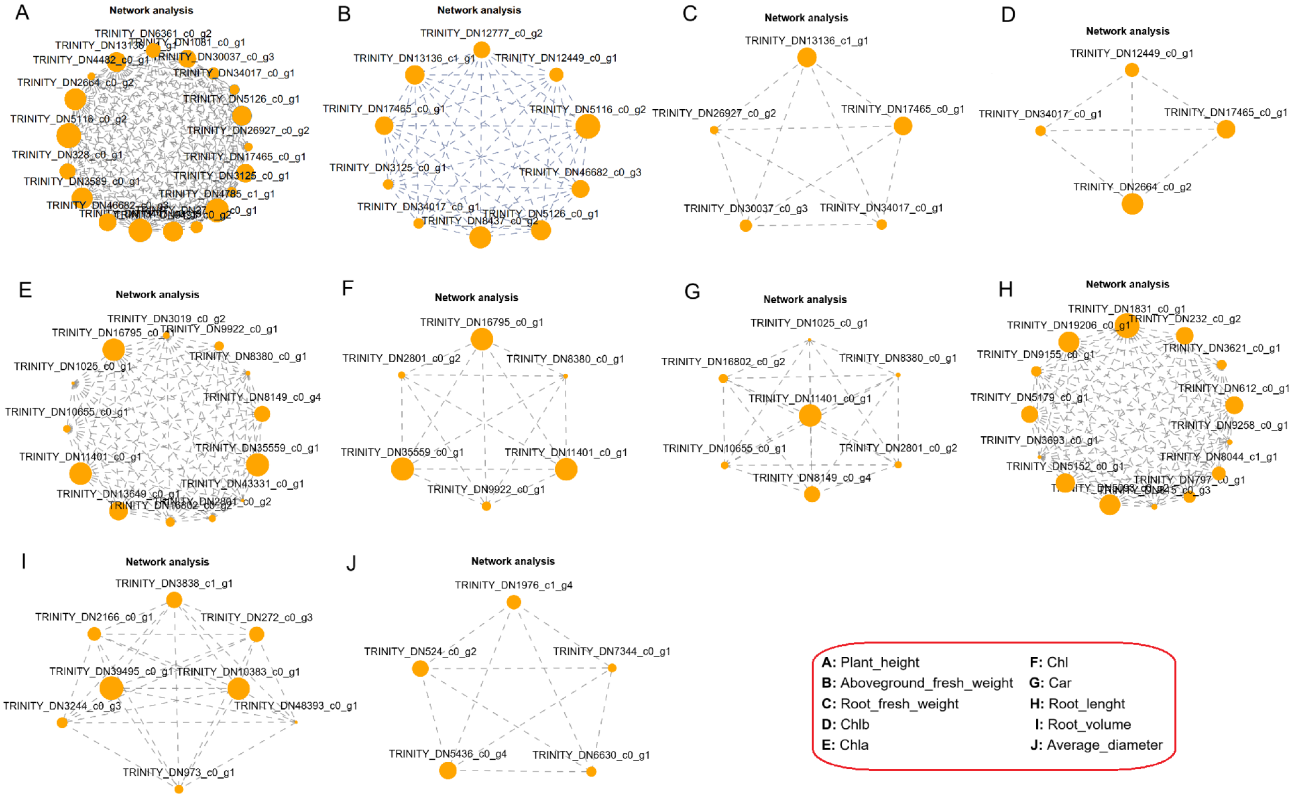

Fig. 10 Network analysis. (**A**) The gene regulatory network for plant height. (**B**) The gene regulatory network for aboveground fresh weight. (**C**) The gene regulatory network for root fresh weight. (**D**) The gene regulatory network for Chlb. (**E**) The gene regulatory network for Chla. (**F**) The gene regulatory network for Chl. (**G**) The gene regulatory network for Car. (**H**) The gene regulatory network for root length. (**I**) The gene regulatory network for root volume. (**J**) The gene regulatory network for average diameter

of gene expression changes in plants under abiotic stress, the analysis of stress regulatory networks, and the identification of key genes [18]. In this study, RNA-seq high-throughput sequencing technology was utilized to obtain a total of 89.41 Gb data, and 94,903 unigenes and 172,374 transcripts were assembled (Table S1). Under high temperature stress, we observed 8,352 DEGs up-regulated and 9,201 DEGs down-regulated in HT_LSL_vs_CK_LSL, compared to 5,433 DEGs up-regulated and 6,325 DEGs down-regulated in HT_MDG_vs_CK_MDG (Fig. 5). Moreover, in HT_LSL_vs_HT_MDG, we found 5,100 DEGs up-regulated and 5,724 DEGs down-regulated (Fig. 5). These DEGs provided important information for further exploring the key genes involved in the response of *P. palustre* to heat stress. It was noteworthy that the number of up-regulated and down-regulated DEGs in MDG was significantly lower than that in LSL after high-temperature stress, indicating that there were significant differences in gene expression levels between MDG and LSL.

Hub genes involved in the response of *P. palustre* to high-temperature stress

In this study, WGCNA further identified 61 hub genes closely related to the response of high-temperature stress in *P. palustre*, including peroxidase 51-like (*TRINITY_DN34017_c0_g1*), NAC domain-containing protein 1 (NAC, *TRINITY_DN328_c0_g1*), UGT73A13 (*TRINITY_DN8437_c0_g2*), UDP-glucuronate 4-epimerase 1-like (GAE1, *TRINITY_DN815_c0_g3*), universal stress protein 7 (USP7, *TRINITY_DN6361_c0_g2*), malonyl-coenzyme: anthocyanin 5-O-glucoside-6'''-O-malonyltransferase-like (5MaT1, *TRINITY_DN3589_c0_g1*), ent-kaurene synthase 5 (KSL5, *TRINITY_DN5126_c0_g1*), ABC transporter (*TRINITY_DN39495_c0_g1*, *TRINITY_DN10383_c0_g1*), etc. (Fig. 11). Plant peroxidases can be classified into three categories based on their substrates: glutathione peroxidase (GPX), ascorbate peroxidase (APX), and guaiacol peroxidase (PPOD) [24]. Among them, GPX and APX can scavenge reactive oxygen species such as H_2O_2, ·OH, and $·O_2^-$ generated during plant growth and development [25–26], playing an important role in resisting stress conditions. NACs play critical roles in enhancing plant heat tolerance by regulating protein localization, forming protein complexes, and

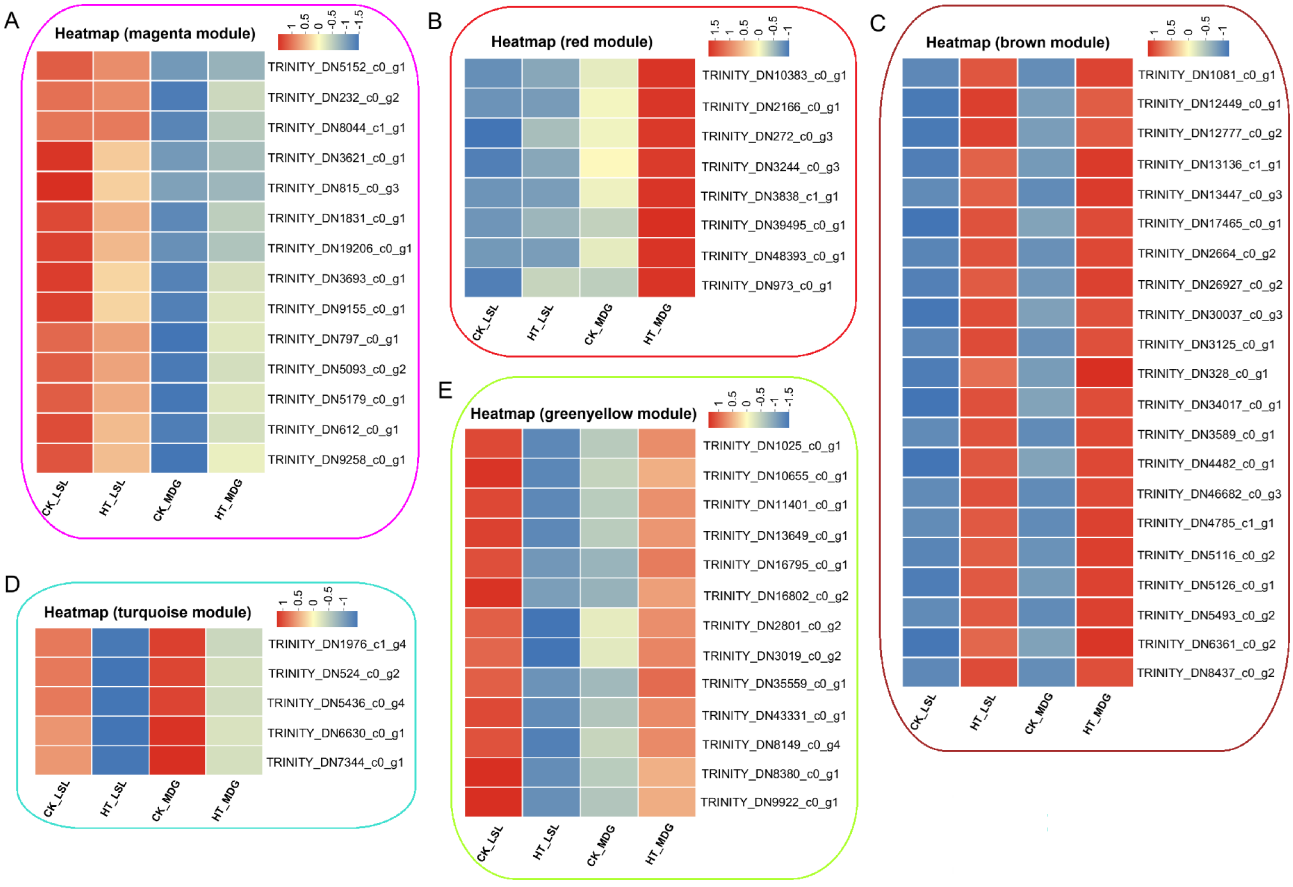

Fig. 11 The expression of hub genes in different modules. (**A**) The expression of hub genes in magenta module. (**B**) The expression of hub genes in red module. (**C**) The expression of hub genes in brown module. (**D**) The expression of hub genes in turquoise module. (**E**) The expression of hub genes in greenyellow module

controlling the expression of heat stress-responsive genes [27]. Xi et al. [28] demonstrated that over-expression of *ZmNAC074* in transgenic *Arabidopsis* can up-regulate the expression levels of antioxidant-related genes (*GPXs* and *APXs*) under heat stress treatments. In this study, peroxidase 51-like (*TRINITY_DN34017_c0_g1*) and NAC (*TRINITY_DN328_c0_g1*) were found to be hub genes and up-regulation, thus we inferred that NAC may regulate the expression levels of peroxidase 51-like to cope with the heat stress.

Diterpenes, also known as diterpenoids, are the most complex and abundant plant metabolites. Over 7,000 compounds are classified as labdane-type diterpenes, and they usually perform significant functions in primary metabolism as basic plant growth hormones like gibberellin (GAs) and in secondary metabolism such as phytoalexins. As the evolutionary precursors of labdane-type diterpenes, GAs are widely found in higher plants, and are required for many aspects of plant growth and development, including seed germination, leaf expansion, stem elongation, and flower development [29]. The homologs of ent-kaurene synthase (KS) in rice are responsible for the biosynthesis of GAs and various phytoalexins, and *OsKSL1* and *OsKSL2* may play an important role in controlling plant height. Additionally, *OsKSL5* was preferentially expressed in the root and significantly inducible expression after two days of GA treatment [30]. In the present study, the diterpenoid biosynthesis pathway was dramatically enriched (Fig. 8D) and may be involved in heat temperature stress responses in *P. palustre*. Moreover, ent-kaurene synthase 5 (*KSL5*, *TRINITY_DN5126_c0_g1*), as a hub gene, was significantly up-regulated under high-temperature stress in both MDG and LSL (Fig. 11), meanwhile, the plant height of *P. palustre* significantly decreased after high-temperature stress (Fig. 2A). Therefore, we speculated that high-temperature stress induced up-regulation of *KSL5* expression in the diterpenoid biosynthesis pathway, which suppressed plant height (response to high-temperature stress) by regulating gibberellin content.

Anthocyanins are a class of plant flavonoids and many of which are modified by malonyl group (s) [31]. Malonyl-CoA: anthocyanin 5-O-glucoside-6‴-O-malonyltransferase of *Salvia splendens* flowers (*Ss5MaT1*) is a member

of the anthocyanin malonyltransferase family that catalyzes the regiospecific transfer of the malonyl group from malonyl-CoA to the 6‴-hydroxyl group of the 5-glycosyl moiety of anthocyanins [32]. In a study on rice, researchers identified and characterized a quantitative trait locus, GSA1, encoding a UDP-glucosyltransferase (UGT83A1), which exhibits glucosyltransferase activity towards flavonoids and monolignols [33]. GSA1 is required for the redirection of metabolic flux from lignin biosynthesis to flavonoid biosynthesis under abiotic stress and the accumulation of flavonoid glycosides, which protect rice against abiotic stress. GSA1 overexpression results in larger grains and enhanced abiotic stress tolerance [33]. In our investigation, the flavonoid biosynthesis pathway was significantly enriched (Fig. 8D) and may be involved in heat stress responses in *P. palustre*. Additionally, UGT73A13 (*TRINITY_DN8437_c0_g2*) possessed a complete open reading frame (ORF) and exhibited significantly elevated expression levels (fold change > 7) in both MDG and LSL following heat stress exposure, and the expression of malonyl-coenzyme: anthocyanin 5-O-glucoside-6‴-O-malonyltransferase-like (5MaT1, *TRINITY_DN3589_c0_g1*) was also increased (Fig. 11). So, it was indicated that high temperature induced up-regulation of *5MaT1* and *UGT73A13* expression, responding to high-temperature stress by regulating flavonoid content.

Universal stress protein (USP) is significantly over-expressed under unfavorable environmental stresses, such as heat/cold shock, oxidative stress, heavy metal toxicity, etc [34]. Plants over-expressing *AtUSP* show strong resistance to heat shock and oxidative stress, compared with wild-type and *Atusp* knock-out plants, confirming the crucial role of *AtUSP* in stress tolerance [35]. In this study, heat stress induced a significantly increased expression of USP7 (*TRINITY_DN6361_c0_g2*) in both MDG and LSL, indicating it might be involved in response to heat stress in *P. palustre*. In *Arabidopsis thaliana*, six *AtGAEs* have been identified. The *gae1 gae6* double mutant exhibits reduced pectin content in the cell walls, increased leaf brittleness, and decreased resistance to specific strains of *Botrytis cinerea* [36]. This seems to suggest a positive correlation between GAE, pectin content, and plant resistance. Meanwhile, a study has shown that high-temperature stress can decrease the pectin content in plants [37]. In *P. palustre*, pectin, or is a polysaccharide, is an important quality evaluation indicator [38], and GAE is a key enzyme in the biosynthesis of polysaccharides in *P. palustre*. In this study, high temperature induced significant down-regulation of GAE gene expression in LSL, but slightly up-regulated expression in MDG. The data presented earlier in this study suggested that MDG may be more heat-resistant than LSL, which meant that MDG may have higher pectin content. However, we also found that GAE was down-regulated in CK_MDG_vs_CK_LSL. Therefore, the relationship among GAE gene expression, pectin content, and heat tolerance in *P. palustre* may be an interesting topic that requires further experimental verification.

In this study, we employed two distinct *P. palustre* varieties (LSL and MDG) to investigate the mechanisms underlying their response to high-temperature stress through comprehensive analysis at both physiological and transcriptomic levels. The research identified key genes intricately associated with heat response in *P. palustre*, thereby laying the foundation for future thermotolerance breeding of this species.

Materials and methods

Plant materials

Two varieties of *P. palustre* (LSL and MDG, originating from Guangxi and Guangdong, respectively) were used as experimental materials and planted at the scientific research base of the Guangxi Botanical Garden of Medicinal Plants. In October 2023, *P. palustre* cuttings with approximately uniform length and stem diameter were taken for hydroponic cultivation (One-quarter strength Hoagland's solution, https://www.coolaber.com). All cuttings were initially per-cultured on a balcony until rooting and then placed in an incubator for high-temperature treatment under the conditions of a diurnal temperature of 38 °C/32°C. The control group was maintained at a diurnal temperature of 28 °C/26°C, with a light-dark cycle of 14 h/10 h and a light intensity of 15,000 lx.

Agronomic trait measurement

One week after the high-temperature treatment, 10 plants of *P. palustre* with basically consistent growth were collected to measure their agronomic traits, including plant height, aboveground fresh weight, and root fresh weight.

Root scanning

The roots of at least 8 plants of *P. palustre* were taken for root scanning using a plant image analyzer system (Microtek, MRS-9600TFU2L, China).

Photosynthetic pigment measurement

The determination of chlorophyll a, chlorophyll b, and carotenoid content referred to the literature by Huang et al. [2].

RNA extraction, library preparation, and sequencing

The fourth to fifth stems from the top of the *P. palustre* plant were collected for transcriptome sequencing. Total RNA was extracted from the tissue using an MJZol total RNA extraction kit (Shanghai Majorbio Bio-pharm Biotechnology Co., Ltd). Then RNA quality was determined by 5300 Bioanalyser (Agilent) and quantified using the

ND-2000 (NanoDrop echnologies). Only high-quality RNA sample was used to construct the sequencing library.

mRNA purification, reverse transcription, library construction, and sequencing were conducted at Shanghai Majorbio Bio-pharm Biotechnology Co., Ltd. (Shanghai, China) according to the manufacturer's instructions (Illumina, San Diego, CA). The RNA-seq transcriptome library was prepared following Illumina® Stranded mRNA Prep, Ligation (San Diego, CA) using 1 μg of mRNA. The sequencing library was performed on the NovaSeq X Plus platform (PE150) using the NovaSeq Reagent Kit (Illumina, San Diego, CA, USA).

Quality control and de Novo assembly

The raw paired-end reads were trimmed and underwent quality control using fastp [39] with default settings. (1) Remove adapter sequences from reads and discard insert-free reads caused by adapter self-ligation or other factors; (2) Trim low-quality bases (quality score < 20) from the 3' end of sequences. Discard the entire read if any remaining base has a quality score < 10; otherwise retain it; (3) Filter out reads containing > 10% ambiguous bases (N); (4) Discard sequences shorter than 20 bp after adapter removal and quality trimming. Subsequently, the cleaned data from the samples were utilized for de novo assembly with Trinity [40]. To increase the assembly quality, all the assembled sequences were filtered using CD-HIT [41] and TransRate [42] and assessed with BUSCO [43]. The assembled transcripts were queried against the NR, COG, and KEGG [44] databases using Diamond to identify proteins with the highest sequence similarity. A cut-off E-value of less than 1.0×10^{-5} was applied to retrieve functional annotations. The BLAST2GO [45] program was employed to obtain GO annotations for unique assembled transcripts, describing biological processes, molecular functions, and cellular components.

Differential expression analysis and functional enrichment

To identify differentially expressed genes (DEGs) between two distinct samples/groups, we calculated the expression level of each transcript using the transcripts per million reads (TPM) method. Gene abundances were quantified using RSEM [46]. Differential expression analysis was conducted using DESeq2 [47]. DEGs with $|\log2FC| \geq 1$ & P-adjust < 0.05 were considered to be significantly different expressed genes. Furthermore, functional enrichment analysis, including GO and KEGG, was performed to identify DEGs significantly enriched in GO terms and metabolic pathways at a Bonferroni-corrected P-value < 0.05, compared to the whole-transcriptome background. GO functional enrichment analysis was carried out using Goatools, while KEGG pathway analysis was conducted using Python's scipy software (https://scipy.org/).

WGCNA

To identify potential high-temperature-responsive modules, the weighted gene coexpression network analysis (WGCNA) package in R was used to construct the coexpression network. After filtering out genes that were expressed at low level, a total of 28,157 genes were selected and imported into WGCNA. The WGCNA network construction and module detection were conducted using an unsigned type of topological overlap matrix (TOM) with a soft-thresholding power β of 4 ($R^2 > 0.8$), a minimal module size of 30, a merge cut height of 0.25, and a minKMEtoStay 0f 0.3. To identify biologically significant modules, module eigengenes were used to calculate correlation coefficients with physiological and biochemical traits by Pearson correlation.

qPCR validation

To ascertain the accuracy of our transcriptome data, we chose seven DEGs potentially associated with high-temperature stress response in *P. palustre* for qPCR validation. The primers used for qPCR are listed in Supplementary Table S6. We followed the reaction system and amplification protocol outlined in Tang et al. [48] for our qPCR experiments.

Supplementary Information

The online version contains supplementary material available at https://doi.org/10.1186/s12870-025-06686-5.

Supplementary Material 1

Supplementary Material 2

Acknowledgements

This research was supported by the Guangxi Key R&D Plan Project (GuikeAB24010015), Fund Projects of the Central Government in Guidance of Local Science and Technology Development (GuiKeZY22096020), National Natural Science Foundation of China (82260750 and 82460754), and Guangxi Qihuang Scholars Training Program (GXQH202402).

Author contributions

Xiufang Li and Fan Wei: Writing-original draft and Data analysis. Changqian Quan and Meihua Xu: Data collection, Visualization, and Formal analysis. Danfeng Tang: Conceptualization, Writing-original draft, Writing-review & editing, Funding acquisition. All authors reviewed the manuscript.

Funding

This research was supported by the Guangxi Key R&D Plan Project (GuikeAB24010015), Fund Projects of the Central Government in Guidance of Local Science and Technology Development (GuiKeZY22096020), National Natural Science Foundation of China (82260750 and 82460754), and Guangxi Qihuang Scholars Training Program (GXQH202402).

Data availability

The transcriptome sequencing data from this paper can be found in the National Center for Biotechnology Information (NCBI) (SRA, accession number, PRJNA1231565).

Declarations

Ethics approval and consent to participate
Not applicable.

Consent for publication
Not applicable.

Competing interests
The authors declare no competing interests.

Received: 13 March 2025 / Accepted: 7 May 2025
Published online: 24 May 2025

References

1. Huang S, Chen H, Wei F, Quan C, Xu M, Chen Z, Li J, Li H, Shi L, Tang D. Comparative analysis of organic and compound fertilizers on the yield and metabolites of *Platostoma palustre*. Phyton-Int J Exp Bot. 2024;93(10):2645–62.
2. Huang Y, Quan C, Wei F, Tang D. Optimal light intensity and photoperiod for the growth and quality of *Platostoma palustre* in a plant factory. J Anim Plant Sci-Pak. 2024;34(5):1257–66.
3. Huang S, Wei X, Quan C, Xu M, Chen Z, Wei F, Tang D. Genetic diversity evaluation and germplasm identification of *Mesona chinensis* Benth from plant morphology, cytology, and ESTSSR molecular markers. Acta Physiol Plant. 2024;46:98.
4. Zhu H, Liao Y, Shi Q. Microscopic identification of *Mesona chinensis* Benth. J Chin Med Mater. 2003, (01), 16–7.
5. Jiangsu New Medical College. Chinese Materia Medica Dictionary. Shanghai: Shanghai People's Publishing House. 1957, 1915.
6. Chen X, Xiao W, Shen M, Yu Q, Chen Y, Yang J, Xie J. Changes in polysaccharides structure and bioactivity during *Mesona chinensis* Benth storage. Curr Res Food Sci. 2022;5:392–400.
7. Tang W, Shen M, Xie J, Liu D, Du MX, Lin L, Gao H, Hamaker B, Xie M. Physicochemical characterization, antioxidant activity of polysaccharides from *Mesona chinensis* Benth and their protective effect on injured NCTC-1469 cells induced by H_2O_2. Carbohyd Polym. 2017;175:538–46.
8. Tang D, Quan C, Lin Y, Wei K, Qin S, Liang Y, Wei F, Miao J. Physio-Morphological, biochemical and transcriptomic analyses provide insights into drought stress responses in *Mesona chinensis* Benth. Front Plant Sci. 2022;13:809723.
9. Tang D, Lin Y, Wei F, Quan C, Wei K, Wei Y, Cai Z, Kashif M, Miao J. Characteristics and comparative analysis of *Mesona chinensis* Benth Chloroplast genome reveals DNA barcode regions for species identification. Funct Integr Genomic. 2022;22(4):467–79.
10. Chen H, Huang SH, Quan CQ, Xu MH, Chen ZN, Wei F, Tang DF. Effects of different colors of plasticfilm mulching on soil temperature, yield, and metabolites in *Platostoma palustre*. Sci Rep-UK. 2024;14:5110.
11. Mahalingam R, Phenotypic. Physiological and malt quality analyses of US barley varieties subjected to short periods of heat and drought stress. J Cereal Sci. 2017;76:199–205.
12. Wang LB. The study on response mechanism and screening of key factors under drought and high temperature stresses in Soybean (*Glycine max* (L.) Merrill). 2018.
13. Qi XY, Wang WL, Hu SQ, Liu MY, Zheng CS, Sun XZ. Effects of exogenous melatonin on photosynthesis and physiological characteristics of chrysanthemum seedlings under high temperature stress. Ying Yong Sheng Tai Xue Bao. 2021;32(7):2496–504.
14. Vollenweider P, Günthardt-goerg MS. Diagnosis of abiotic and biotic stress factors using the visible symptoms in foliage. Environ Pollut. 2006;140(3):562–71.
15. Wang CX, Wang YY, Lin F, Wu SL, Lin KL. Key techniques for high-yield cultivation of mesona chinensis. Contemp Hortic. 2010;03:47–8.
16. Yao H, Zhong YQ. Cultivation techniques of *Mesona chinensis*. Contemp Hortic. 2014, (02), 52.
17. Huo ZG, Zhang HY, Li CH, Kong R, Jiang MY. Review on high temperature heat damage of maize in China. J Appl Meteorological Sci. 2023;34(1):1–14.
18. Xu XF. Transcriptome and proteome analysis of maize leaf under high temperature stress. 2019.
19. Mu XY, Ma ZY, Zhang LX, Fu J, Liu TX, Ding Y, Xia LK, Zhang FQ, Zhang J, Qi JS, Zhao X, Tang BJ. Responses of photosynthetic fluorescence characteristics, pollination, and yield components of maize cultivars to high temperature during flowering. Chin J Eco-Agriculture. 2022;30(1):57–71.
20. Zhao BX, Zhang YC, Zhou L, Yang LY, Yao JJ, Huang QJ. Research progress on high temperature stress of *Rosa hybrida*. North Hortic. 2021;10:124–31.
21. Feng XJ, Yu ZN, Guo HR, Zhang ZS, Zeng RZ, Xie L. Research progress in the effect of high temperature stress on the growth and development of *Anthurium andraeanum*. Ecol Sci. 2021;40(02):218–24.
22. Zhao LF, Li CH, Liu TX, Wang XP, Pan X. Genotypic responses and physiological mechanisms of maize (*Zea mays* L.) to high temperature stress during flowering. Acta Agron Sinica. 2012;38(5):857–64.
23. Wardlaw IF, Moncur L, Patrick JW. The response of wheat to high temperature following anthesis. Li. Sucrose accumulation and metabolism by isolated kernels. Funct Plant Biol. 1995;22(3):399–407.
24. Meng YY, Fan SL, Song MZ, Pang CY, Yu SX. Advance in research on class III peroxidases and its function in plants. Acta Bot Boreali-Occidentalia Sinica. 2011;31(9):1908–16.
25. Qiao XR, Zhang JY. Research progress on GPX in plants. Biotechnol Bull. 2016;32(9):7–13.
26. Li HH, Lai ZX. A review of progress in ascorbate peroxidase in plants. Subtropical Plant Sci. 2006;2:66–9.
27. Xiong H, He H, Chang Y, Miao B, Liu Z, Wang Q, Dong F, Xiong L. Multiple roles of NAC transcription factors in plant development and stress responses. J Integr Plant Biol. 2025;00:1–29.
28. Xi Y, Ling Q, Zhou Y, Liu X, Qian Y. ZmNAC074, a maize stress responsive NAC transcription factor, confers heat stress tolerance in Transgenic *Arabidopsis*. Front Plant Sci. 2022;13:986628.
29. Yang M, Liu G, Yamamura Y, Fu J. Identification and functional characterization of ent-kaurene synthase gene in *Ilex latifolia*. Beverage Plant Res. 2021;1:7.
30. Teng Y, Wang Y, Zhang Y, Xie Q, Zeng Q, Cai M, Chen T. Genome-wide identification and expression analysis of ent-kaurene synthase-like gene family associated with abiotic stress in rice. Int J Mol Sci. 2024;25:5513.
31. Suzuki H, Nakayama T, Yonekura-Sakakibara K, Fukui Y, Nakamura N, Nakao M, Tanaka Y, Yamaguchi M-a, Kusumi T, Nishino T. Malonyl-CoA: anthocyanin 5-O-Glucoside-6‴-O-Malonyltransferase from Scarlet Sage (*Salvia splendens*) flowers: enzyme purification, gene cloning, expression, and characterization. J Biol Chem. 2001;276(52):49013–9.
32. Suzuki H, Nakayama T, Nishino T. Proposed mechanism and functional amino acid residues of Malonyl-CoA: anthocyanin 5-O-Glucoside-6‴-O-Malonyltransferase from flowers of *Salvia splendens*, a member of the versatile plant acyltransferase family. Biochemistry. 2003;42(6):1764–71.
33. Dong NQ, Sun Y, Guo T, Shi CL, Zhang YM, Kan Y, Xiang YH, Zhang H, Yang YB, Li YC, Zhao HY, Yu HX, Lu ZQ, Wang Y, Ye WW, Shan JX, Lin HX. UDP-glucosyltransferase regulates grain size and abiotic stress tolerance associated with metabolic flux Redirection in rice. Nat Commun. 2020;11(1):1–16.
34. Chi YH, Koo SS, Oh HT, Lee ES, Park JH, Phan KAT, Wi SD, Bae SB, Paeng SK, Chae HB, Kang CH, Kim MG, Kim WY, Yun DJ, Lee SY. The physiological functions of universal stress proteins and their molecular mechanism to protect plants from environmental stresses. Front Plant Sci. 2019;10:750.
35. Jung YJ, Melencion SMB, Lee ES, Park JH, Alinapon CV, Oh HT, Yun DJ, Chi YH, Lee SY. Universal stress protein exhibits a redox-dependent chaperone function in *Arabidopsis* and enhances plant tolerance to heat shock and oxidative stress. Front Plant Sci. 2015;6:1141.
36. Bethke G, Thao A, Xiong G, et al. Pectin biosynthesis is critical for cell wall integrity and immunity in Arabidopsis thaliana. Plant Cell. 2016;28(2):537–56.
37. Lima RB, dos Santos TB, Vieira LGE, de Lourdes LFM, Ferrarese-Filho O, Donatti L, Boeger MRT, de Oliveira Petkowicz CL. Heat stress causes alterations in the cell-wall polymers and anatomy of coffee leaves (Coffea Arabica L). Carbohydr Polym. 2013;93:135–43.
38. Tang D, Quan C, Huang S, Wei F, Integrating LC-MS. HS-GC-MS for the metabolite characterization of the Chinese medicinal plant *Platostoma palustre* under different processing methods. Front Nutr. 2023;10:1181942.
39. Chen S, Zhou Y, Chen Y, Gu J. Fastp: an ultra-fast all-in-one FASTQ preprocessor. Bioinformatics. 2018;34(17):i884–90.
40. Grabherr MG, Haas BJ, Yassour M, Levin JZ, Thompson DA, Amit I, et al. Full-length transcriptome assembly from RNA-Seq data without a reference genome. Nat Biotechnol. 2011;29:644–52.
41. Fu LM, Niu BF, Zhu ZW, Wu ST, Li WZ. CD-HIT: accelerated for clustering the next-generation sequencing data. Bioinformatics. 2012;28(23):3150–2.
42. Smith-Unna R, Boursnell C, Patro R, Hibberd JM, Kelly S. TransRate: reference-free quality assessment of de Novo transcriptome assemblies. Genome Res. 2016;26(8):1134–44.

43. Mosè M, Berkeley MR, Seppey M, Simão FA, Zdobnov EM. BUSCO update: novel and streamlined workflows along with broader and deeper phylogenetic coverage for scoring of eukaryotic, prokaryotic, and viral genomes. Mol Biol Evol. 2021;38(10):4647–54.
44. Kanehisa M, Goto SKEGG. Kyoto encyclopedia of genes and genomes. Nucleic Acids Res. 2000;28:27–30.
45. Conesa A, Gotz S, Garcia-Gomez JM, Terol J, Talon M, Robles M. Blast2GO: a universal tool for annotation, visualization and analysis in functional genomics research. Bioinformatics. 2005;21:3674–6.
46. Li B, Dewey CN. RSEM: accurate transcript quantification from RNA-Seq data with or without a reference genome. BMC Bioinformatics. 2011;12:323.
47. Love MI, Huber W, Anders S. Moderated Estimation of fold change and dispersion for RNA-seq data with DESeq2. Genome Biol. 2014;15(12):550.
48. Tang D, Huang Q, Wei K, Yang X, Wei F, Miao J. Identification of differentially expressed genes and pathways involved in growth and development of *Mesona chinensis* Benth under red- and blue-light conditions. Front Plant Sci. 2021;12:761068.

Publisher's note